Metallurgy

Tanju Teker* and Murat Sarı

Metallurgical properties of boride layers formed in pack boronized cementation steel

https://doi.org/10.1515/mt-2022-0098

Abstract: In the present study, cementation steel was exposed to boronizing process at 950 °C for 6, 8, and 10 h. Microstructural changes on the surface of the samples after boron operation were inspected by optical microscope, scanning electron microscope, energy-dispersive spectroscopy, X-ray diffraction, electron back-scatter diffraction, and elemental mapping analysis. In addition, surface roughness, microhardness, and boride layer thicknesses were measured. The boride layers deposited on the cementation steel consisted either single or double phases. The level of boride deposit of all samples was achieved from 90 to 156 μm. The boride layer created at 950 °C for 10 h involved the FeB and Fe_2B. The boride layers had a much higher hardness value than the substrate material due to the presence of FeB and Fe_2B.

Keywords: boronizing; cementation steel; microhardness; microstructure; surface roughness.

1 Introduction

Industrial boron treatment is generally employed for ferrous alloys. Since the boronizing process is a diffusion-based process, the temperature is the main parameter for this process; therefore, the boronizing process is also applied at high temperatures to generate the boride deposits on the surface of iron-based alloys. Therefore, temperature plays a critical role to achieve the desired boron layer thickness. A single-phase (Fe_2B) or a double-phase boride layer (Fe_2B and FeB) occurs on the surface of steels that are commonly widely used in the industry [1–3]. However, according to the chemical content of the substrate material, the content of the boride layers may also contain different elements. The FeB component forms at the upper layer of the substrate material, whereas the Fe_2B component takes place below the FeB layer. It is desired that the surface of the boronized material forms from a single-deposit Fe_2B component. This is because Fe_2B and FeB components have different volume and coefficient of thermal expansion, which causes cracks and breaks on the surface of boronized material after boron treatment [4–7]. Since the generation of the free energy level of the boride deposit is negative, the chemical and thermal stability of the boride deposits are excellent. Accordingly, compared to other diffusion-based coating techniques (carburizing and nitriding), boron deposits have a harder structure. In addition, boride layers formed on the material surfaces have two main interests on the mechanical properties of the materials. The first effect is high hardness, which also increases the wear resistance. The second one is the sawtooth morphology, which provides the interaction between the substrate material and the boron layer improves [8–10]. Li et al. [11] observed the effects of boriding temperature and time on the microstructure and wear resistance of Cr12Mn2V2. The high temperature and long processing time produced excellent wear resistance.

In this study, the effect of the boron procedure time on the boride deposits created at 950 °C process temperature for 6, 8, and 10 h processing time was experimentally investigated.

2 Experimental approach

The cementation steel was exposed to the boronizing treatment at 950 °C for 6, 8, and 10 h. Later, the boronized samples were flatted by 200–1200 mesh sand paper, and then polished by 1–3 μm diamond solution. Ekabor II (5 wt% B_4C and 90 wt% SiC) was dehumidified at 100 °C for 24 h. As indicated in Figure 1, the samples were inserted in the pot. Afterward, to perform the boron treatment, the samples were heated up at 950 °C for 6, 8, and 10 h by a digitally controlled Protherm brand furnace. After boron treatment, the samples were prepared for metallographic examination. Changes occurring in the microstructure

***Corresponding author: Tanju Teker**, Department of Manufacturing Engineering, Faculty of Technology, Sivas Cumhuriyet University, Sivas 58140, Turkey, E-mail: tanjuteker@cumhuriyet.edu.tr
Murat Sarı, Department of Manufacturing Engineering, Faculty of Technology, Sivas Cumhuriyet University, Sivas 58140, Turkey

were examined by an optical microscope (LEICA DM750), a scanning electron microscope (SEM: ZEISS EVO LS10) equipped with an energy-dispersive spectrometer (EDS), electron back-scatter diffraction (EBSD), and elemental mapping analysis. The chemical phase composition was determined by Rigaku brand X-ray diffraction (XRD) at 40 kV, 40 mA, CuKα radiation. The microhardness test was performed under a 30 g load using QNESS Q10M tester. Mitutoyo SJ-210 model device was utilized to measure the surface roughness values of the boronized samples.

3 Results and discussion

3.1 Microstructure evaluation of boride coating

Optical and SEM images of the samples exposed to boronizing at 950 °C for 6, 8, and 10 h are shown in Figures 2 and 3. As stated in the literature, after boron treatment, there were three different zones in the microstructure such as boride layer, transition region, and base metal [12, 13]. The presence of alloying elements such as chromium, vanadium, and carbon had an opposite effect on the boride deposit thickness. Also, it was understood that the growth direction of the layer was toward the substrate material. Boron atoms were relatively small and had high mobility. Therefore, they diffused easily from the surface to the substrate material. As can be seen from the optical and SEM photographs, dense and compact structures were formed on the substrate material surface after boron treatment. Besides, the transition zones were clearly visible. The morphology and the level of the boride deposits could change according to the chemical content of the substrate material.

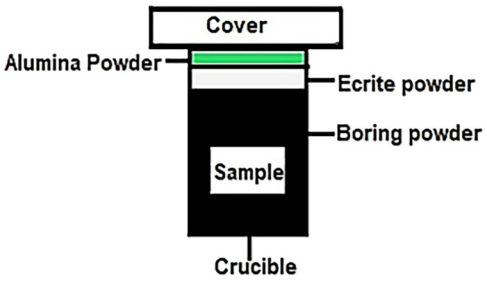

Figure 1: Arrangement of the samples into the pot.

The level of the boride deposit formed at 950 °C for 10 h was more than the sample boronized for 8 h. The level of the boride deposit formed at 950 °C for 8 h was higher than of the sample boronized for 6 h. As seen in SEM photographs, accordingly, the boride deposit thicknesses were measured as 90.92 μm for 6 h, 102.68 μm for 8 h, and 156.55 μm for 10 h. Consequently, an increase in the thickness of the boride deposit was detected with the increasing process time. Throughout the boron treatment, boride deposit growth was observed in columnar form due to anisotropic diffusion of boron atoms. In stainless steel or iron-based alloys, the alloying elements concentrated at the tips of the boride deposits prevented the diffusion of the boron atom into the substrate material. As a result, a microstructure similar to saw tooth was manufactured between the layer and the substrate material. Due to the increase in the boron potential of the boronizing media (boron atoms activated in the Ekabor powder), increasing the process time incremented the thickness of the boride layer. The boron treatment time of 10 h favored a thicker boride layer than that of 8 h due to the higher reaction time of the boron atoms. The boron atoms released from Ekabor powders, then, started diffusing and reacted in order to form more Fe_2B at the Fe_2B–alloy interface. As can be seen from the SEM photographs, the Fe_2B layer thickness was not uniform on the surface of all samples. This was because the diffusion path was not the same for all samples. The thinner the Fe_2B layer at a certain location, the shorter the diffusion path. Also, the proportion of boron atoms dispersed at that location was high. The Fe_2B layer grew faster in thinner regions than in thicker regions. Martini et al. [14] stated that the alloying element was likely to play a negative role on the growth mechanism of iron borides. The alloying elements slow the growth kinetics of boron layers since they concentrate at the tips of boride layers, slowing boron diffusion in some regions, which means that it reduces boron layer columnarity in substrate material [15, 16]. A single-phase Fe_2B compound is more desirable when compared to an FeB compound on the coating. The FeB phase was undesirable on the surface of the samples because it has higher boron content and a very hard and brittle structure. It was determined that there were cracks on the surfaces of the boron layers for all samples due to the distinction in the thermal expansion coefficients of the FeB and Fe_2B compounds formed on the surfaces. Especially in areas with FeB phase, the cracks occurred due to high stress. The EDS analyses of the sample boronized at 950 °C for 10 h are given in Figure 4. The EDS analyses confirmed the effect of the reaction

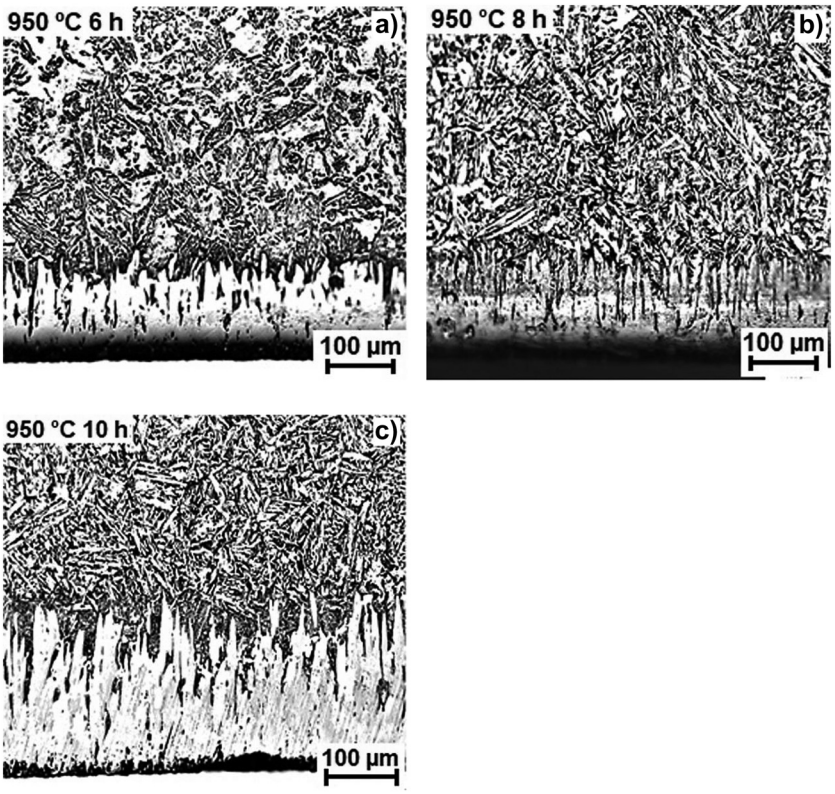

Figure 2: Optical images of boronized samples at 950 °C for a) 6, b) 8, and c) 10 h.

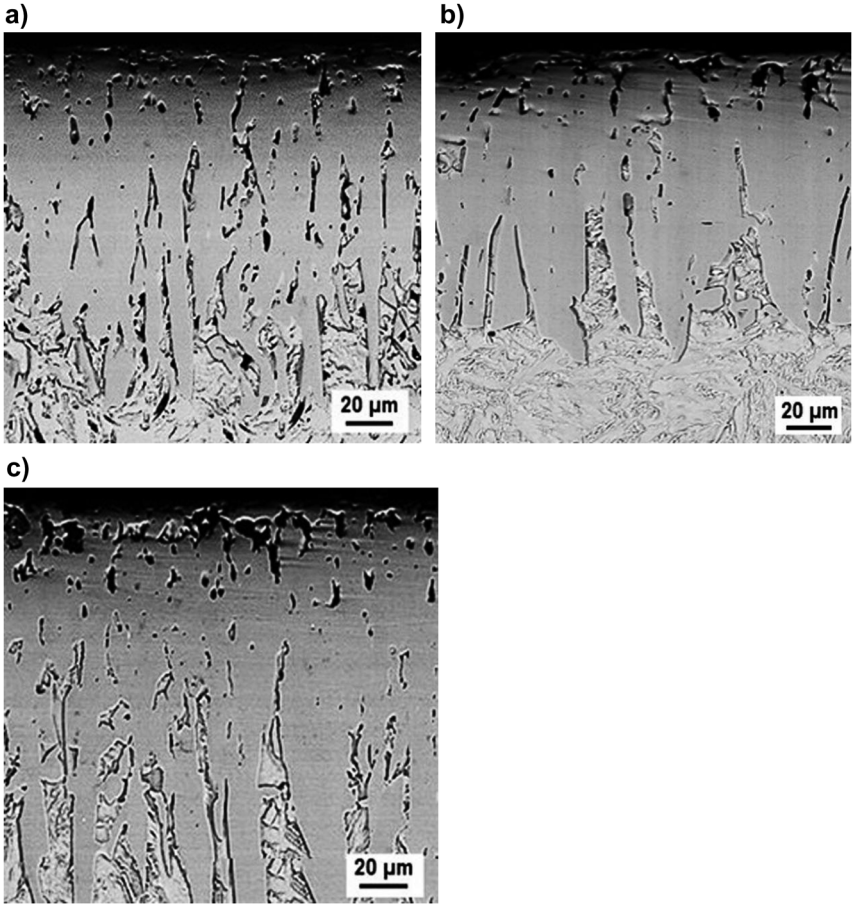

Figure 3: Scanning electron microscopy images of boronized samples at 950 °C for a) 6, b) 8, and c) 10 h.

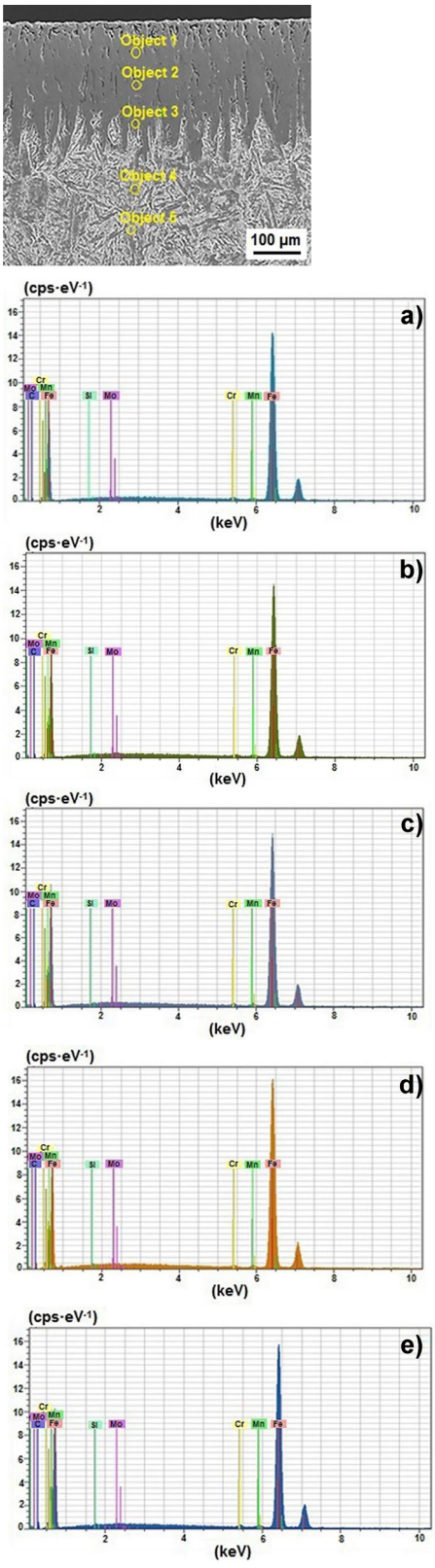

Figure 4: Energy-dispersive spectroscopy analyses of the sample boronized for 10 h at 950 °C. The SEM-EDS points and analyses of the sample boronized at 950 °C for 10 h are given in Figure 4a–e.

time. It was seen that the Fe_2B phase penetrated to a deeper region in the boride deposit and transition zone.

3.2 Hardness

The hardness–distance values of cementation steels boronized at 6, 8, and 10 h at 950 °C are given in Figure 5. The microhardness of the base metal of the sample boronized for 6 h at 950 °C was 160 HV, whereas that of the boride layer of the same sample was 1200 HV. The microhardness of the base metal of the sample boronized for 8 h was 180 HV, whereas that of the boride layer was 1260 HV. Although the microhardness value of the base metal of the sample boronized for 10 h was 230 HV, the microhardness of the boride layer was 1310 HV. It was seen that there was an increase in microhardness values with increasing reaction time. In the present study, boride layers having double-phase (FeB and Fe_2B) were observed for all samples. It was stated that alloying elements such as nickel and chromium in steels produce high surface tension between the boride layer and the base metal, which had a negative effect on the sawtooth morphology. This was because while chromium can easily be dissolved in boride layers, nickel does not tend to dissolve in the boride layer [16]. Throughout the boron treatment, the alloying elements in steels were likely to tend to redistribute depending on the solubility, temperature, and reaction time. Therefore, the mechanical properties of the substrate material and the boride layer were significantly modified. The alloying elements were likely to affect the diffusion of boron atoms and the interface between the coating and the base metal. Long reaction time and high processing temperature created a thicker boride layer on the substrate material surface [17].

Most studies showed that the microstructure and strength properties of the boride layer depend on the chemical rate of the substrate material [18, 19]. The distribution of nonuniform boron atoms in the boride layers increased the pore formation in the boride layers, which affect the mechanical properties negatively. The boride layers containing compounds with two different hardness scales were obtained for all samples. The sample exposed to boron treatment for 10 h had the highest hardness values, whereas the sample exposed to boron treatment for 6 h had the lowest hardness values. The average hardness of the boride layers was about 1310 HV. The boride layers had a much higher hardness value than the substrate material due to the presence of FeB and Fe_2B compounds. Also, the hardness range for the same sample fluctuated in

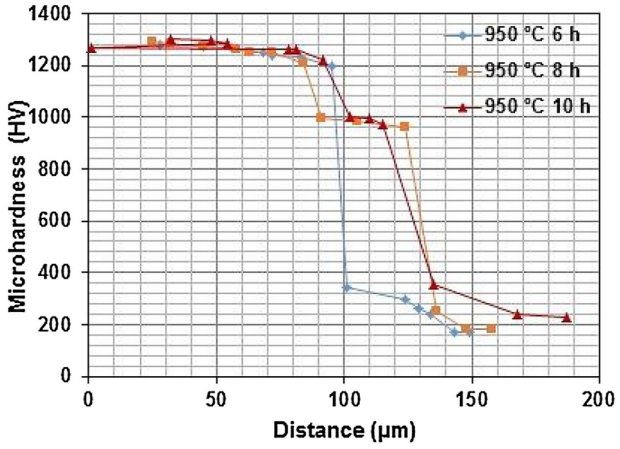

Figure 5: Hardness-distance values of sample boronized for 6, 8, and 10 h at 950 °C.

a narrow area, which was a sign of the existence of structural flaws and pores in the boride layers.

3.3 XRD analysis

The presence of components in boride layers was confirmed by XRD analysis. The XRD analysis graph of cementation steel boronized at 950 °C for 8 h is shown in Figure 6. The Fe_2B phase was seen as the main phase as a result of boron treatment for 8 h. Although boride layer crystals grow toward the substrate material, they meet many obstacles. As a result, the growth of the increased boride layer crystal becomes kinetically difficult into the substrate material [19]. The new boride layers' crystals that occurred in the transition zone were pushed to expand with their axis vertical to the outer surface. It was found that the intensity of the Fe_2B phase peak was decreased with increasing reaction time. The XRD analysis of the sample

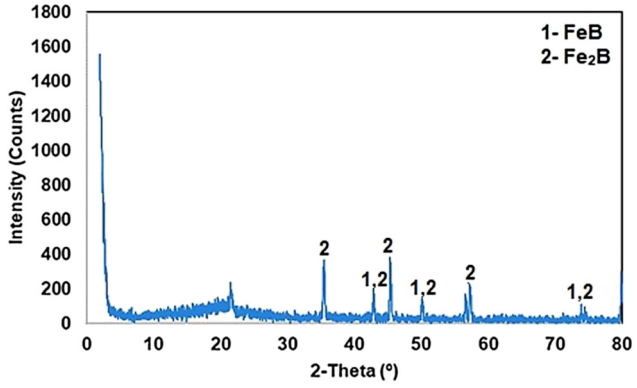

Figure 6: X-ray diffraction analysis graph of cementation steel boronized for 10 h at 950 °C.

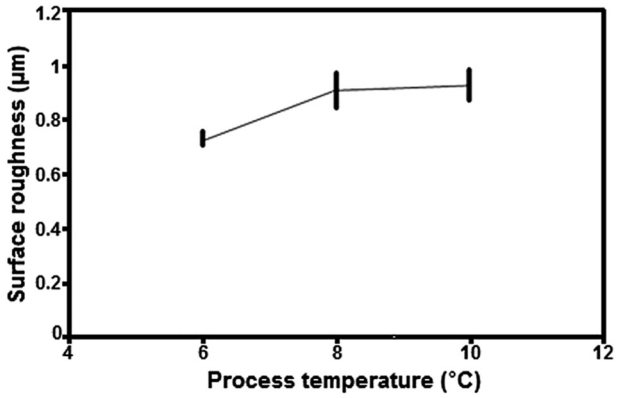

Figure 7: Surface roughness analysis results of samples boronized for 6, 8, and 10 h.

exposed to boron treatment for 8 h showed that the peak of the Fe_2B phase was intensified. The intensities of the FeB phase were also weak or they disappeared. This was most likely attributed to low boron potential in the boronizing process.

3.4 Surface roughness analysis

The surface roughness analysis results of samples boronized for 6, 8, and 10 h are shown in Figure 7. The surface roughness value of the sample boronized for 6 h was measured as 0.75 µm, the surface roughness rate of the sample boronized for 8 h was 0.90 µm, and the surface roughness value of the sample boronized for 10 h was 1.00 µm. An increase in surface roughness occurred with increasing reaction time. The average surface roughness value of samples boronized at a processing temperature of 950 °C for 6, 8, and 10 h was measured, which was 0.88 µm. In the area between the base metal and the FeB layer, there was no pore or void, whereas there were pores and voids in the area between the Fe_2B and the FeB layers.

3.5 Elemental mapping analysis

Elemental mapping analysis of samples boronized at 950 °C for 10 h is given in Figure 8. In the substrate material, there were many zones having different alloying elements and iron concentrations, which were the main element of the matrix but especially, the surfaces of all samples after boron treatment had intense zones having boron (B). Elements such as Mn, Cr, C, Mo, and Si found as alloying elements in cementation steel were also determined. In the integrity to the boronized layer, the extent and the quantity

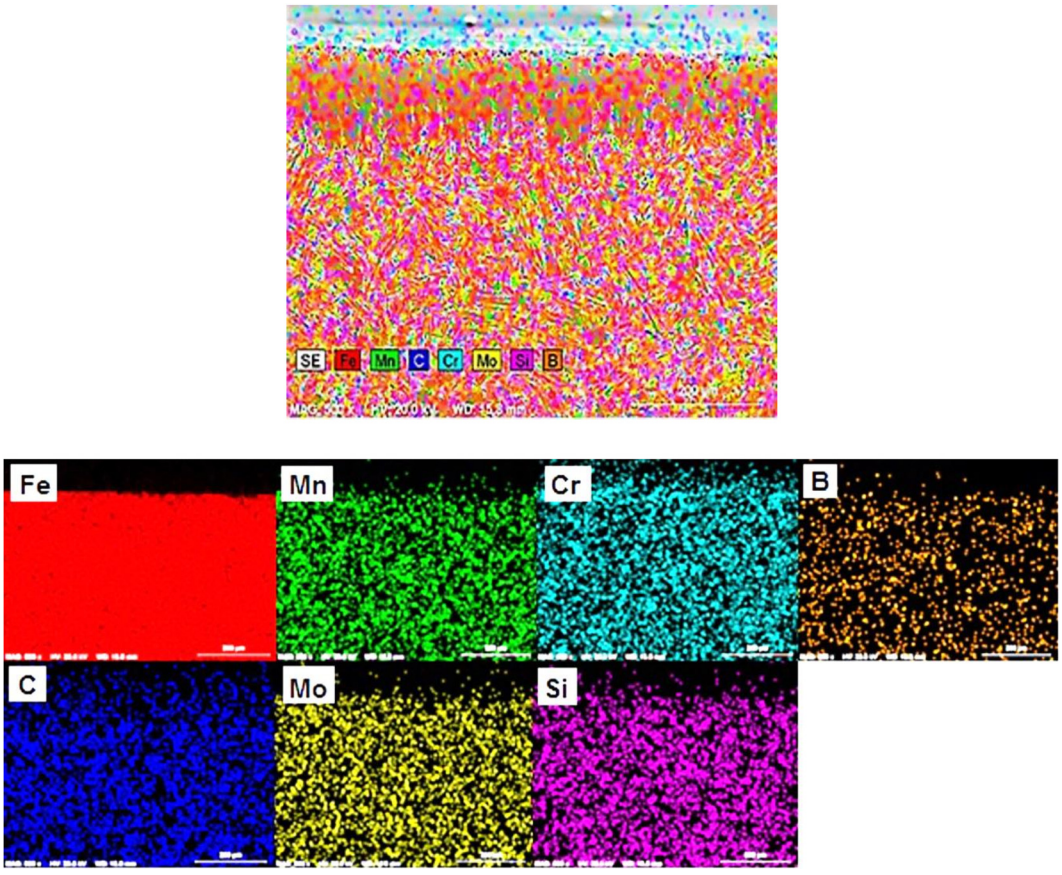

Figure 8: Elemental mapping analysis of cementation steel boronized for 10 h.

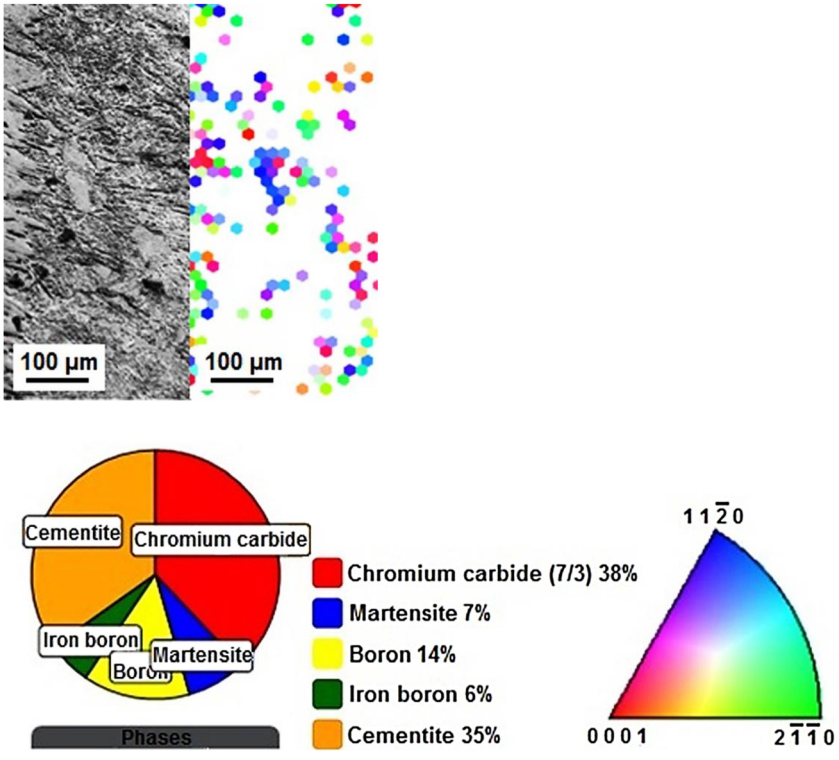

Figure 9: Electron back-scatter diffraction analysis results of the sample boronized for 10 h.

of particles increased quickly. This represented that their type would be concerned with the carbon distribution from the boronized layer toward the parent material. It was accepted that the carbon was nearly exactly insolvable in boride layers [19–21]. Thus, it disseminated from the surface into the base alloy.

3.6 EBSD analysis

The EBSD analysis results of the sample boronized at 10 h are given in Figure 9. As a result of boron treatment, 14 wt% boron, 6 wt% iron–boron, 35 wt% cementite, 8 wt% martensite, and 38 wt% chromium carbides were formed in the boride layer and substrate material. The Fe_2B boride layer was the first compound occurring on all the sample surfaces. This boride layer began to form with the interaction between the cementation steel surface and Ekabor powders. The growth morphology of the boride layer was in the acicular form due to the existence of an easiest direction. There were many obstacles during the growth of the Fe_2B layers. Still, boride crystal layers were forced to grow into the substrate material. Consequently, the novel boride crystals occurring at the boride layer–substrate material interface was regularly pressed to increase their axis vertical to the exterior surface, i.e., aligned to the boron incline in the samples, leading to an Fe_2B preferential inducement that progressively resisted on going toward the interface with the substrate.

4 Conclusions

The effect of the boron procedure time on the boride layer created at 950 °C process temperature for 6, 8, and 10 h processing time was experimentally investigated.

- The coating layer (boride layer) generally consisted FeB (outer layer) and Fe_2B (inner layer) components. The boride layers formed on all sample surfaces did not have a homogenous distribution.
- The microhardness of the boride layer increased according to the reaction time, and the boride layers exhibited a higher microhardness value when compared to that of the substrate material.
- The activity of the boron on the cementation surface was related to the growth rate of the layers and reaction time. The reaction time played a crucial role on the boride layer thickness.
- There were no cracks or inhomogeneities in the area between the layer and the substrate.
- After boron treatment, 14 wt% boron, 6 wt% iron boron, 35 wt% cementite, 7 wt% martensite, and 38 wt% chromium carbides were formed in the coating layer and substrate.

Author contributions: All the authors have accepted responsibility for the entire content of this submitted manuscript and approved submission.
Research funding: This research was carried out under Grant Number: 2018/0002 of Adıyaman University Scientific Research Projects Unit.
Conflict of interest statement: The authors declare no conflicts of interest regarding this article.

References

[1] Z. N. Abdellah, B. Boumaali, and M. Keddam, "Computer simulation of boronizing kinetics for a TB2 alloy," *Mater. Test.*, vol. 63, no. 12, pp. 1130–1135, 2021, https://doi.org/10.1515/mt-2021-0051.
[2] V. Jain and G. Sundararajan, "Influence of the pack thickness of the boronizing mixture on the boriding of steel," *Surf. Coat. Technol.*, vol. 149, no. 1, pp. 21–26, 2002, https://doi.org/10.1016/S0257-8972(01)01385-8.
[3] S. Aich and K. S. Ravi Chandran, "TiB whisker coating on titanium surfaces by solid-state diffusion: synthesis, microstructure, and mechanical properties," *Metall. Mater. Trans. A*, vol. 33, pp. 3489–3498, 2012, https://doi.org/10.1007/s11661-002-0336-6.
[4] X. Tian, Y. L. Yang, S. J. Sun, J. An, Y. Lu, and Z. G. Wang, "Tensile properties of boronized N80 steel tube cooled by different methods," *J. Mater. Eng. Perform.*, vol. 18, pp. 162–167, 2009, https://doi.org/10.1007/s11665-008-9270-0.
[5] N. Gidikova, "Vanadium boride coatings on steel," *Mater. Sci. Eng. A*, vol. 278, nos. 1–2, pp. 181–186, 2000, https://doi.org/10.1016/S0921-5093(99)00596-1.
[6] C. H. Xu, J. K. Xi, and W. Gao, "Improving the mechanical properties of boronized layers by superplastic boronizing," *J. Mater. Process. Technol.*, vol. 65, nos. 1–3, pp. 94–98, 1997, https://doi.org/10.1016/0924-0136(95)02247-3.
[7] J. Li and B. Li, "Preparation of the TiB_2 coatings by electroplating in molten salts," *Mater. Lett.*, vol. 61, no. 6, pp. 1274–1278, 2007, https://doi.org/10.1016/j.matlet.2006.07.007.
[8] U. Fastner, T. Steck, A. Pascual, G. Fafilek, and G. E. Nauer, "Electrochemical deposition of TiB_2 in high temperature molten salts," *J. Alloys Compd.*, vol. 452, no. 1, pp. 32–35, 2008, https://doi.org/10.1016/j.jallcom.2007.02.130.
[9] M. Kulka and A. Pertek, "Microstructure and properties of borided 41Cr4 steel afterlaser surface modification with re-melting," *Appl. Surf. Sci.*, vol. 214, nos. 1–4, pp. 278–288, 2003, https://doi.org/10.1016/S0169-4332(03)00500-2.
[10] X. C. Xin and O. Menglan, "A mechanical explanation for the influence of residual stress on the wear resistance of borided steel," *Wear*, vol. 137, no. 2, pp. 151–159, 2010, https://doi.org/10.1016/0043-1648(90)90132-T.

[11] C. Li, B. Shen, G. Li, and C. Yang, "Effect of boronizing temperature and time on microstructure and abrasion wear resistance of Cr12Mn2V2 high chromium cast iron," *Surf. Coat. Technol.*, vol. 202, pp. 5882–5886, 2008, https://doi.org/10.1016/j.surfcoat.2008.06.170.
[12] G. Rodríguez-Castro, I. Campos-Silva, J. Martínez-Trinidad, U. Figueroa-López, D. Meléndez-Morales, and J. Vargas-Hernández, "Effect of boriding on the mechanical properties of AISI 1045 steel," *Adv. Mater. Res.*, vol. 65, pp. 63–68, 2009, https://doi.org/10.4028/www.scientific.net/AMR.65.63.
[13] K. Bartsch and A. Leonhardt, "Formation of iron boride layers on steel by d.c.-plasma boriding and deposition processes," *Surf. Coat. Technol.*, vols. 116–119, pp. 386–390, 1999, https://doi.org/10.1016/S0257-8972(99)00078-X.
[14] C. Martini, G. Palombarini, and M. Carbucicchio, "Mechanism of thermochemical growth of iron borides on iron," *J. Mater. Sci.*, vol. 39, pp. 933–937, 2004, https://doi.org/10.1023/B:JMSC.0000012924.74578.87.
[15] L. G. Yu, X. J. Chen, K. A. Khor, and G. Sundararajan, "FeB/Fe_2B phase transformation during SPS pack-boriding: boride layer growth kinetics," *Acta Mater.*, vol. 53, no. 8, pp. 2361–2368, 2005, https://doi.org/10.1016/j.actamat.2005.01.043.
[16] I. Campos, J. Oseguera, U. Figueroa, J. A. García, O. Bautista, and G. Kelemenis, "Kinetic study of boron diffusion in the paste-boriding process," *Mater. Sci. Eng. A*, vol. 352, nos. 1–2, pp. 261–265, 2003, https://doi.org/10.1016/S0921-5093(02)00910-3.
[17] O. Allaoui, N. Bouaouadja, and G. Saindernan, "Characterization of boronized layers on a XC38 steel," *Surf. Coat. Technol.*, vol. 201, no. 6, pp. 3475–3482, 2006, https://doi.org/10.1016/j.surfcoat.2006.07.238.
[18] M. Keddam and S. M. Chentouf, "A diffusion model for describing the bilayer growth (FeB/Fe_2B) during the iron powder-pack boriding," *Appl. Surf. Sci.*, vol. 252, no. 2, pp. 393–399, 2005, https://doi.org/10.1016/j.apsusc.2005.01.016.
[19] J. Lubas, "Tribological properties of surface layer with boron in friction pairs," *Surf. Rev. Lett.*, vol. 16, no. 5, pp. 767–773, 2006, https://doi.org/10.1142/S0218625X09013232.
[20] I. Campos, G. Ramirez, U. Figueroa, J. Martinez, and O. Morales, "Evaluation of boron mobility on the phases FeB, Fe_2B and diffusion zone in AISI 1045 and M2 steels," *Appl. Surf. Sci.*, vol. 253, no. 7, pp. 3469–3475, 2007, https://doi.org/10.1016/j.apsusc.2006.07.046.
[21] T. Teker and E. M. Karakurt, "Characterization of the boron layer formed by pack boronizing of binary iron-niobium alloys," *Mater. Test.*, vol. 61, no. 9, pp. 875–879, 2019, https://doi.org/10.3139/120.111396.

The authors of this contribution

Tanju Teker
Prof. Dr. Tanju Teker, born in Sivas in 1971, works in Sivas Cumhuriyet University, Faculty of Technology, Department of Manufacturing Engineering, Sivas, Turkey. He graduated in Metallurgy Education from the Gazi University, Ankara, Turkey, in 1997. He received his M.Sc. and Ph.D. degrees from the Firat University, Elazig, Turkey, in 2004 and 2010, respectively. His research interests include metal coating techniques, casting, fusion welding, and solid-state welding method.

Murat Sarı
Murat Sarı was born in Ankara in 1991. He graduated from the Adıyaman University, Faculty of Engineering, Department of Metallurgy and Materials Engineering, Adıyaman, Turkey, in 2017. He received his M.Sc. degree from the Adıyaman University, Adıyaman, Turkey, in 2019. His research interests include metal coating techniques and welding methods.